Stem Cell Reports
Resource
OPEN ACCESS

Non-genetic Purification of Ventricular Cardiomyocytes from Differentiating Embryonic Stem Cells through Molecular Beacons Targeting IRX-4

Kiwon Ban,[1,6] Brian Wile,[2,6] Kyu-Won Cho,[1,6] Sangsung Kim,[1] Ming-Ke Song,[3] Sang Yoon Kim,[1] Jason Singer,[4] Anum Syed,[2] Shan Ping Yu,[3] Mary Wagner,[4] Gang Bao,[2,*] and Young-sup Yoon[1,5,*]
[1]Department of Medicine, Division of Cardiology, Emory University School of Medicine, Atlanta, GA 30322, USA
[2]Department of Biomedical Engineering, Georgia Institute of Technology and Emory University, Atlanta, GA 30322, USA
[3]Department of Anesthesiology, Emory University School of Medicine, Atlanta, GA 30322, USA
[4]Department of Pediatrics, Emory University School of Medicine and Children's Healthcare of Atlanta, Atlanta, GA 30322, USA
[5]Severance Biomedical Science Institute, Yonsei University College of Medicine, Seoul 120-752, Korea
[6]Co-first author
*Correspondence: gang.bao@rice.edu (G.B.), yyoon5@emory.edu (Y.-s.Y.)
http://dx.doi.org/10.1016/j.stemcr.2015.10.021

SUMMARY

Isolation of ventricular cardiomyocytes (vCMs) has been challenging due to the lack of specific surface markers. Here we show that vCMs can be purified from differentiating mouse embryonic stem cells (mESCs) using molecular beacons (MBs) targeting specific intracellular mRNAs. We designed MBs (IRX4 MBs) to target mRNA encoding Iroquois homeobox protein 4 (*Irx4*), a transcription factor specific for vCMs. To purify mESC vCMs, IRX4 MBs were delivered into cardiomyogenically differentiating mESCs, and IRX4 MBs-positive cells were FACS-sorted. We found that, of the cells isolated, ~98% displayed vCM-like action potentials by electrophysiological analyses. These MB-purified vCMs continuously maintained their CM characteristics as verified by spontaneous beating, Ca^{2+} transient, and expression of vCM-specific proteins. Our study shows the feasibility of isolating pure vCMs via cell sorting without modifying host genes. The homogeneous and functional ventricular CMs generated via the MB-based method can be useful for disease investigation, drug discovery, and cell-based therapies.

INTRODUCTION

Heart failure is the leading cause of death worldwide; however, current therapies such as surgical interventions are capable only of delaying the progression of this devastating disease (Go et al., 2013). In particular, patients suffering from myocardial infarction (MI), a major cause of heart failure, have cardiac dysfunction due to significant loss of cardiomyocytes (CMs) (Laflamme and Murry, 2011). The adult mammalian heart has very limited ability to regenerate after such a loss.

Due to their self-renewal and multi-lineage differentiation capacity, embryonic stem cells (ESCs) and induced pluripotent stem cells (iPSCs), collectively called pluripotent stem cells (PSCs), have emerged as a highly promising and renewable source for generating CMs (Kehat et al., 2001; Laflamme et al., 2007; Yang et al., 2008; Zwi et al., 2009). Studies have shown that cell cultures directed toward differentiation into CMs include three types of CMs, nodal, atrial, and ventricular CMs, in varying ratios as well as other lineage cells (Huber et al., 2007; Lian et al., 2012; Shiba et al., 2012; Tohyama et al., 2013). Each type of cardiac-chamber-specific CM has unique functional, structural, and electrophysiological characteristics (Ng et al., 2010). Thus, transplantation of cardiomyogenically differentiated cells, which include heterogeneous CMs and other lineage cells, into injured myocardium might induce dysrhythmia, asynchronous cardiac contraction, or aberrant tissue formation (Liao et al., 2010). Since ventricular CMs are the most extensively affected cell type in MI and the major source for generating cardiac contractile forces, there has been great interest in producing ventricular CMs from stem cells for treatment of MI (Bizy et al., 2013; Lee et al., 2012; Müller et al., 2000; Zhang et al., 2011). It would therefore be ideal to generate a pure population of ventricular CMs from PSCs for cardiac-cell-based therapies.

Despite the unmet medical need, to date, no studies have demonstrated the feasibility of isolating ventricular CMs without permanently altering their genome. Prior studies used genetic modification for isolating ventricular CMs by inserting a fluorescent reporter gene driven by the MYL2 (or MLC-2v) promoter into mouse ESCs and embryonic carcinoma cell lines (Bizy et al., 2013; Lee et al., 2012; Müller et al., 2000; Zhang et al., 2011). Such genetic modification precludes clinical use of the isolated cells due to concerns of tumorigenicity or adverse reactions. These ventricular CMs would not be appropriate for drug development or disease modeling due to the random and permanent changes in the genome or the use of viral vectors. Further, there are no known surface markers specific for ventricular CMs, disallowing antibody-based cell sorting with flow cytometry, which is the most common method for isolating targeted cells from differentiating PSCs.

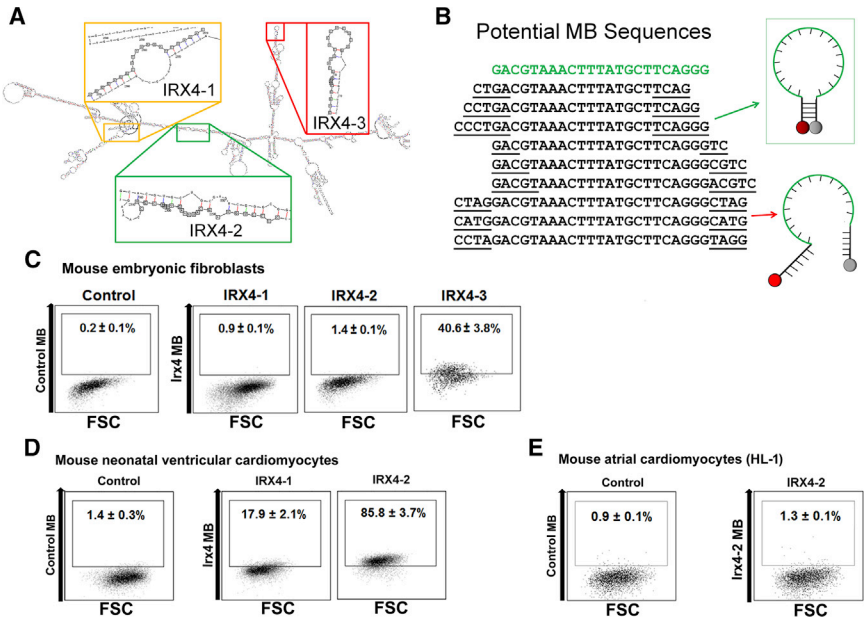

Figure 1. Selection of Optimal Ventricular Cardiomyocyte-Specific IRX4 Molecular Beacons

(A) *Irx4* mRNA structure was predicted using the RNAfold web server. Three unique target sequences were identified in *Irx4* mRNA that maximized the number of predicted unpaired bases as well as the binding affinity of a complementary probe.

(B) Stem sequences were appended to the complementary sequence and evaluated using QUIKFOLD to minimize the free energy that causes the oligonucleotide to assume a hairpin structure in solution.

(C–E) Flow cytometry results after delivering various IRX4 MBs designed to identify Irx4 mRNAs, or control MB, into mouse embryonic fibroblasts (C), eonatal mouse ventricular CMs (D), and HL-1 CMs (E). The number in each panel represents the percentage of fluorescent cells. FSC indicates forward scatter. All experiments were performed on three independent biological replicates (C–E).

Although not surface markers, several genes are known to be specifically expressed in ventricular hearts or CMs. As a ventricular-specific transcription factor, Iroquois homeobox protein 4 (IRX4) has been reported to be exclusively expressed in the ventricular myocardium while absent from both atria and the outflow tract (Bao et al., 1999). IRX4 positively regulates ventricular-chamber-specific gene expression by activating the ventricular myosin heavy chain-1 (VMHC1) gene while suppressing the expression of atrial myosin heavy chain-1 (AMHC1) (Bruneau et al., 2000; Wang et al., 2001). As a structural protein, MYL2 (or MLC-2v), one of the essential MLC-2 isoforms that is important for the contractile function of ventricular CMs, is expressed in ventricular CMs (Marionneau et al., 2005; O'Brien et al., 1993). MYL2 expression is mostly restricted to the ventricular segment of the heart with minimal expression in the outflow track during cardiogenesis (Kubalak et al., 1994; O'Brien et al., 1993).

Accordingly, we have developed a method targeting an intracellular gene to purify ventricular CMs. We used a molecular beacon (MB)-based method for isolating a pure population of ventricular CMs by targeting the mRNA of the ventricular-specific transcription factor IRX4 (Figures 1A and 1B). MBs are 20- to 30-bp oligonucleotide probes with a fluorophore and a quencher at the 5′ and 3′ ends, respectively (Figures 1A and 1B) (Heyduk and Heyduk, 2002). They are designed to form a stem-loop (hairpin) structure so that the fluorophore and quencher are within close proximity and fluorescence is quenched. Hybridization of the MBs with the target mRNA opens the hairpin structure and physically separates the fluorophore from the quencher, allowing a fluorescence signal to be emitted upon excitation (Tsourkas et al., 2002). It has been demonstrated that cellular delivery of MBs does not alter the expression level of the target genes (Rhee and Bao, 2009; Rhee et al., 2008; Santangelo et al., 2006; Tsourkas et al., 2002), and MBs can be used to isolate mESCs by directly targeting specific intracellular mRNAs such as Oct4 (Rhee and Bao, 2009). Further, we demonstrated that MBs enable the enrichment of general CMs from differentiating mouse and human PSCs (Ban et al., 2013).

In the present study, we developed a sophisticated approach using MBs targeting transcription factor mRNAs, which, due to their low copy numbers compared to structural protein mRNAs, are highly challenging and were not previously attempted. By designing specific MBs targeting *Irx4* mRNA, we show here that functional ventricular CMs derived from differentiating mouse ESCs could be isolated with high purity. The MB-based cell isolation method is quite versatile; a wide range of specific intracellular mRNAs could be targeted to achieve high specificity, including mRNAs encoding structural proteins and transcription factors.

RESULTS

Ventricular Cardiomyocyte-Specific Gene Selection

Through an extensive literature search, we selected Irx4 as a target gene for generating ventricular CM-specific MBs (Bao

Table 1. IRX-4 MB Designs

Beacon Design	Beacon Sequence (5′–3′)[a]	Target Sequence (5′–3′)
IRX4-1	*Cy3*-CACCTAGTTTTGTTATATTAGCCTCCCTAGGTG-*BHQ2*	AGGGAGGCTAATATAACAAAAC
IRX4-2	*Cy3*-CCCTGACGTAAACTTTATGCTTCAGGG-*BHQ2*	CCCTGAAGCATAAAGTTTACGTC
IRX4-3	*Cy3*-CAGGCAGAGAGTAGAAAGCAGATGCCTG-*BHQ2*	AGGCATCTGCTTTCTACTCTCTG
Control MB	*Cy3*-ACGACGCGACAAGCGCACCGATACGTCGT-*BHQ2*	GTATCGGTGCGCTTGTCGCG

[a]Underlined bases indicate the arms forming the stem.

et al., 1999; Bruneau et al., 2000; Wang et al., 2001). First, we measured mRNA expression levels of Irx4 via qRT-PCR analysis in CMs isolated from either ventricles or atria of mouse adult hearts. We also measured Myl2, which is a well-defined ventricular CM-specific gene, as a positive control. The results showed that Irx4 was robustly expressed in ventricular CMs, but not atrial CMs (Figure S1A). The expression levels of both Irx4 and Myl2 mRNAs were substantially higher in mouse ventricular CMs compared to atrial CMs, indicating that Irx4 is a viable target for MB selection.

Generation of IRX4 MBs

We designed three IRX4 MBs targeting distinct sites in the mouse Irx4 mRNA using design rules validated in our previous publications (Figures 1A and 1B) (Ban et al., 2013; Rhee et al., 2008; Tsourkas et al., 2002). In addition, we used mFold (Zuker, 2003) and the RNA Composer Webserver (Popenda et al., 2012) to model the IRX4 MB designs and to predict the accessibility of hybridization sites in the target mRNAs. These IRX4 MBs were synthesized with a Cy3 fluorophore on the 5′ end and a Black Hole Quencher 2 (BHQ2) on the 3′ end as specified in Table 1. We quantified MB fluorescence signals when hybridized to perfectly complementary or mismatched synthetic DNA targets by incubating 500-nM MBs in solution with increasing concentrations (60–500 nM) of DNA targets. IRX4 MB signals were recorded using a microplate reader and normalized by the background signals in wells with MBs only. All IRX4 MBs displayed a linear response to increasing concentrations of complementary targets and low signal levels when mismatched targets were used (Figure S1B).

Delivery of MBs into Different Cell Types

After testing several different methods for cellular delivery of MBs, we found that the use of a Nucleofector (Lonza) with Nucleofection Solution V and program A033 was an efficient method (up to 99%) to deliver MBs to a variety of cell types (Ban et al., 2013). To further refine this approach, we also designed two distinct MBs as controls. The first was a non-specific interaction indicator MB (RQ) that contained a 20-bp loop sequence given by random walk, which did not have any perfect matches in the entire mouse genome. Therefore, any fluorescence resulting from this control MB would be non-specific signal. The second was a delivery control MB (UQ) with the same random sequence, but it did not contain a quencher, so it fluoresced at all times. Both RQ and UQ MBs were delivered to cells to ensure that delivery was efficient and that MB signal was specific to the target mRNA sequence.

Selection of Optimal IRX4 MB for Isolating Ventricular-like Cardiomyocytes

In order to select the best MB to efficiently identify and isolate ventricular CMs, we examined the specificity, sensitivity, and reliability of each IRX4 MB in three separate systems. To determine the specificity of MBs, we used nucleofection to deliver each of the three IRX4 MBs into mouse embryonic fibroblasts (mEFs), which do not express IRX4, and analyzed the cells that showed false-positive signals using flow cytometry. We found that among the three MB designs (IRX4-1, IRX4-2, and IRX4-3) examined, IRX4-1 and IRX4-2 MBs yielded significantly fewer false-positive cells from mEFs (IRX4-1: 0.9% ± 0.1%, and IRX4-2: 1.4% ± 0.1%) than IRX4-3 MB (40.6% ± 3.8%). Hence, only IRX4-1 and IRX4-2 MBs were selected for further experiments (Figure 1C). To evaluate the detection sensitivity of IRX4-1 and IRX4-2 MBs, each was delivered into mouse neonatal ventricular CMs and analyzed with flow cytometry. IRX4-2 MBs resulted in a substantially higher percentage of ventricular CMs (85.8% ± 3.7%) compared to IRX4-1 MBs (17.9% ± 2.1%). On the basis of these results, we selected IRX4-2 MB as the probe for enriching mESC-derived ventricular CMs (Figure 1D).

To further confirm detection specificity, we delivered the IRX4-2 MB to HL-1 CMs, an immortalized mouse atrial CM cell line known to retain atrial CM characteristics (Brundel et al., 2006; Claycomb et al., 1998). Flow cytometry analysis showed that less than 2% of HL-1 CMs displayed a positive signal from IRX4-2 MBs, providing additional support for the high specificity of IRX4-2 MB in isolating ventricular CMs (Figure 1E). We also tested the IRX4-2 MB against the most likely contaminating cell types in cardiomyogenically differentiated PSC cultures: mouse smooth muscle

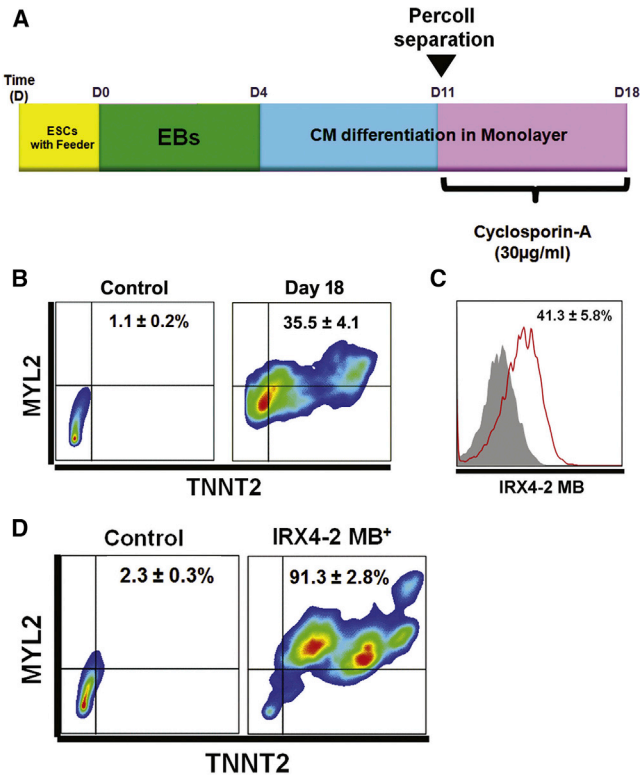

Figure 2. Purification of Ventricular Cardiomyocytes from Differentiating mESCs through IRX4-2 MBs

(A) A schematic of the protocol to differentiate mESCs to the cardiac lineage. ESCs, mouse embryonic stem cells; EBs, embryoid bodies.

(B) Flow cytometric scattergrams showing the percentages of cells expressing both TNNT2 and MYL2 at differentiation day 18.

(C) A flow cytometry plot showing IRX4-2-MB-positive cells at differentiation day 18.

(D) Flow cytometric scattergrams showing the percentages of cells expressing both TNNT2 and MYL2 after FACS sorting with IRX4-2 MB.

All experiments were performed on three (B and D) or six (C) independent biological replicates.

cells (SMCs), mouse aortic endothelial cells (mECs), mouse cardiac fibroblasts (mCFs), and mESCs (Figure S1C). Flow cytometry analysis showed that less than 3% of those cells displayed detectable fluorescence signals. These results clearly demonstrated that the IRX4-2 MB is specific for identifying ventricular CMs.

Generation of Ventricular CMs from Mouse ESCs

To ensure stable production of mESC-derived ventricular CMs, we first established an embryoid body (EB)-mediated CM differentiation system (Figure 2A). Undifferentiated mouse ESCs (J1) maintained on STO feeder cells were enzymatically detached to form EBs. Since EB-induced differentiation alone is not sufficient to produce a high percentage of CMs, we plated day-4 EBs into a fibronectin-coated dish and added ascorbic acid (50 μg/ml) to enhance CM differentiation. Spontaneously beating clumps began to appear 3–4 days after plating (Takahashi et al., 2003) (Movie S1). After 7 days of CM differentiation on monolayer cultures, we enzymatically dissociated the cells and applied them to a discontinuous Percoll gradient (40.5% to 58.5%) to enrich mESC-derived CMs (Xu et al., 2002). Percoll-mediated separation typically produces three layers of cells, and the bottom layer was reported to include a higher percentage of CMs. Thus, the cells in the bottom layer were collected and cultured for another 7 days in the presence of cyclosporine A (30 μg/ml) to further induce CM differentiation (Fujiwara et al., 2011). Finally, we applied IRX4 MBs to these 18-day cultured mESC-derived CMs.

qRT-PCR analysis revealed dynamic changes in the expression of CM-specific genes in our differentiation system, indicative of efficient CM differentiation. Expression of cardiac contractile genes (*Tnnt2* and *Myh7*) and genes for atrial (*Myl7*) and ventricular (*Myl2* and *Irx4*) CMs began to appear 7 days after culture. Expression of *Myl2* and *Irx4* continuously increased until day 18 (Figure S2A).

We next carried out immunocytochemistry and flow cytometry to further characterize the cell population at day 18. Immunocytochemistry demonstrated that day-18 cells significantly expressed CM-specific proteins, including ACTN2 (α-sarcomeric actinin), TNNT2 (cardiac troponin T), and MYH6/7 (α and β myosin heavy chain), confirming their CM nature (Figure S2B). A substantial number of cells that were positive for ACTN2, TNNT2, and MYH6/7 concomitantly expressed MYL2 (or MLC2V), which is a specific protein for ventricular CMs. At day 18, the percentages of cells expressing TNNT2 or MYL2 were 67.9% ± 4.5% and 39.2% ± 3.8%, respectively (Figure S3A), and 35.5% ± 4.1% of cells expressed both TNNT2 and MYL2 (Figure 2B). These results clearly indicate efficient generation of CMs, with a significant percentage of ventricular CMs, through our CM differentiation system.

Purification of mESC-Derived Ventricular CMs through IRX4-2 MBs

After establishing the CM differentiation system, we delivered IRX4-2-MB to the 18-day differentiated cells to isolate ventricular CMs. We used a pre-validated nucleofection protocol to deliver MBs and sorted the cells by fluorescence-activated cell sorting (FACS). Flow cytometry results showed that 41.3% ± 5.8% of cells were positive for fluorescence signal from IRX4-2 MB (Figure 2C). This number is similar to the detection rate (39.2% of Myl2-positive cells) of ventricular CMs using antibody-based methods. We then conducted FACS sorting based on IRX4-2-MB signal, and the MB-positive CMs were seeded

onto fibronectin-coated plates for further experiments. The IRX4-2-MB-positive CMs began to beat spontaneously within 48 hr and continued to beat vigorously for up to 2 weeks (Movie S2). Only a small number of IRX4-2-MB-negative cells showed beating (data not shown).

To determine the cell viability after IRX4-2-MB-based cell sorting, we performed a propidium iodide (PI)-based cell viability assay (Chan et al., 2012; Sasaki et al., 1987). To this end, two groups of cells were treated with PI: one group that underwent FACS sorting with IRX4-2 MB transfection and the other without IRX4-2 MB transfection. Then, we performed flow cytometry to measure the PI-negative, or viable, cells. Flow cytometry analyses showed that ~55.5% of the IRX4-2-MB-transfected group was PI negative as was ~63.4% of the group without IRX4-2 MB transfection (Figure S3B), suggesting ~8% cell damage caused by MBs.

Two days after FACS sorting, we conducted flow cytometry analyses using TNNT2 and MYL2 antibodies to quantify the percentage of CMs and ventricular-like CMs in IRX4-2-MB-positive cells. The percentage of cells expressing either TNNT2 or MYL2 was 97.2% ± 3.4% or 91.6% ± 5.1%, respectively (Figure S3C), and that expressing both TNNT2 and MYL2 was 91.3% ± 2.8% (Figure 2D). Together, these results indicate efficient enrichment of mESC-derived ventricular CMs by IRX4-MB-based cell sorting.

Electrophysiological Characteristics of IRX4 MB+ Ventricular-like CMs

To investigate the electrophysiological characteristics of IRX4-2-MB-positive and -negative CMs, we performed whole-cell patch clamp analyses (Figure 3A). It is known that the action potential duration (APD) is longer in mouse fetal ventricular CMs than in atrial CMs (Figure 3A) (Hume and Uehara, 1985). Similarly, we found that IRX4-2-MB-positive CMs displayed substantially longer APDs than IRX4-2-MB-negative cells (Figure 3A). APD_{50} was also longer in IRX4-2-MB-positive cells than in IRX4-2-MB-negative cells (159 ± 21.7 ms versus 35 ± 7.8 ms, $p < 0.01$) (Figure 3B). On the basis of these results, we found that 98% of IRX4-2-MB-positive cells possessed ventricular type action potentials (APs) (49 out of 50 cells), which showed electrical synchronism, whereas atrial- or nodal-type APs were not observed in these cells (Figure 3C). Due to the small number of contracting cardiomyocytes in the IRX4-2-MB-negative cells, we were unable to appropriately measure the APs. Alternatively, we performed immunostaining to verify the identity of the IRX4-2-MB-negative cells with CM-specific antibodies. Immunocytochemistry demonstrated that none of the IRX4-2-MB-negative cells expressed the ventricular CM marker MYL2, and less than 20% of them expressed ACTN2, suggesting that there are some CMs, but no ventricular CMs, in the IRX4-2-MB-negative population (Figure S4A).

Next, we performed multielectrode arrays (MEAs) to investigate the synchronous activities of the purified CMs. While IRX4-2-MB-negative cells showed limited and non-synchronous electrical activities, IRX4-2-MB-positive CMs demonstrated regular and synchronous APs, suggesting a well-coupled syncytium of cells with appropriate CM electrophysiological characteristics in the IRX4-2-MB-positive population. Lack of electrical activity measured in the IRX4-2-MB-negative cells may be due to a higher proportion of non-CM cell types in this population (Figure S4B).

Last, we performed real-time intracellular calcium $[Ca^{2+}]i$ imaging analysis with IRX4-2-MB-sorted ventricular CMs in comparison to fetal mouse atrial and ventricular CMs (Figures 3D and 3E). In this analysis, all three types of CMs showed automaticity, but the patterns of calcium transients of IRX4-2-MB-positive CMs were similar to ventricular CMs, but not to atrial CMs; the frequency was slower and the amplitude was larger in IRX4-2-MB-positive CMs and ventricular CMs compared to atrial CMs (Figures 3D and 3E). Collectively, these results demonstrated that the IRX4-2-MB-positive cells possess ventricular-CM-like electrophysiological properties.

Cellular Characterization of FACS-Sorted Ventricular CMs

To examine the cardiac identity and homogeneity of the ventricular CMs purified with IRX4-2 MB, immunocytochemistry was conducted with antibodies against various CM-specific markers (ACTN2, TNNT2, and MYH6/MYH7 and MYL2) and a ventricular CM marker (MYL2) 2–3 days after FACS sorting and cell culture. As shown in Figure 4A, immunocytochemistry demonstrated that almost all IRX4-2-MB-isolated ventricular CMs exhibited ACTN2, TNNT2, and MYH6/MYH7. Furthermore, a positive immunoreactivity for MYL2 was found in all of the IRX4-2-MB-positive CMs (Figure 4A). Importantly, these IRX4-2-MB-positive CMs abundantly expressed GJA1 (known as connexin 43), an important connexin isoform in the formation of gap junctions between ventricular CMs, indicating that these enriched ventricular CMs possess the functional capability of forming cardiac junctions (Figure 4B). qRT-PCR analyses further demonstrated that expression of ventricular CM genes *Irx4* and *Myl2* was substantially increased in IRX4-2-MB-positive cells compared to the IRX4-2-MB-negative cells (Figure 4C; Table S1). Furthermore, these IRX4-2-MB-positive cells showed a significant increase in the expression of general CM-specific genes (*Tnnt2* and *Myh6/Myh7*) compared to the IRX4-2-MB-negative cells (Figure 4C). Genes representing atrial-specific CMs (Myl7) or other cell types were either expressed at negligible levels (*Acta2*, *Ddr2*, and *MyoD*) or were non-detectable (*Pecam1* and *Neuro D*) in the IRX4-2-MB-positive cells (Figure 4C and data not shown).

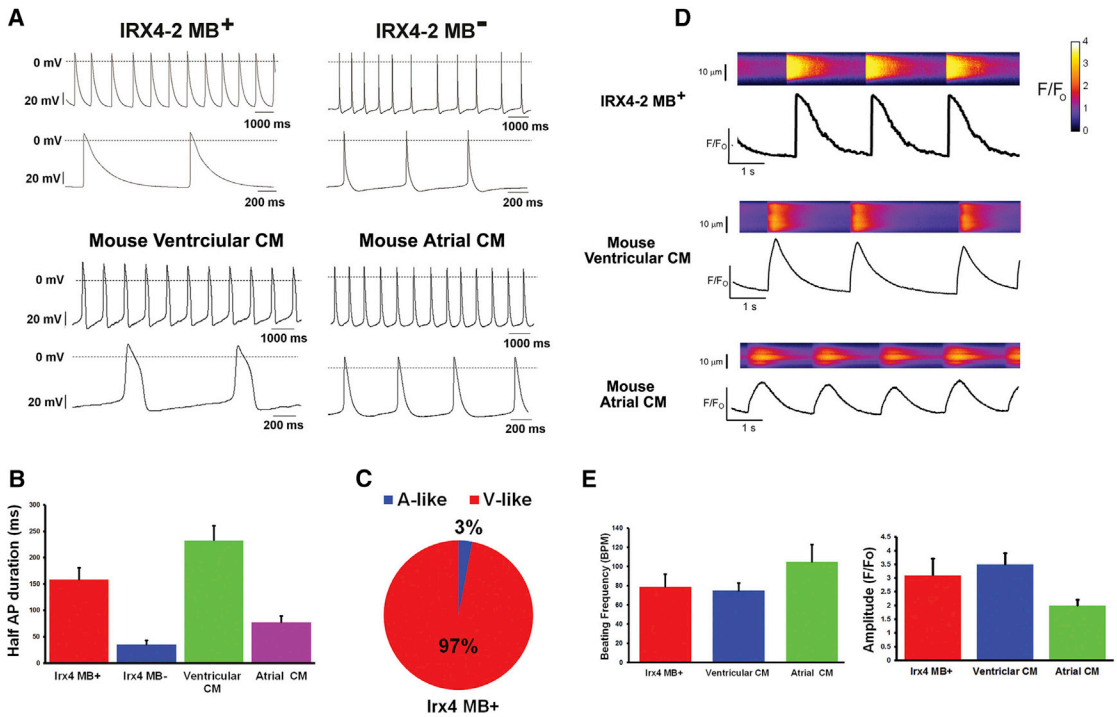

Figure 3. Electrophysiological Characteristics of IRX4-2-MB-Purified Ventricular Cardiomyocytes

(A) Representative action potentials of IRX4-2-MB-positive and -negative cells (upper panel) and primarily isolated mouse fetal ventricular and atrial cardiomyocytes (lower panel).

(B) Half action potential duration (APD_{50}) of IRX4-2-MB-positive and -negative cells and mouse fetal ventricular and atrial cardiomyocytes.

(C) The percentages of the action potential types recorded from IRX4-2-MB-positive cells. A-like, atrial-like AP; V-like, ventricular-like AP. Action potentials were measured from 50 cells in each group (A–C).

(D) Representative spontaneous calcium transients in IRX4-2-MB-positive cardiomyocytes (upper panel), mouse primary fetal ventricular cardiomyocytes (middle panel), and mouse primary fetal atrial cardiomyocytes (lower panel). In each panel, calcium transients were recorded in the upper section, where increasing calcium is indicated by the change in color from dark blue to light blue, and fluorescence intensity was normalized to the baseline measured at time 0 (F_o).

(E) The averages of the beating frequency (BPM) and calcium amplitude (F/F_0) of IRX4-2-MB-positive cells and mouse fetal ventricular and atrial cardiomyocytes.

Calcium transient experiments were performed on 15 cells in each group (D and E).

Taken together, our results clearly demonstrated that IRX4-2 MBs targeting ventricular CM-specific mRNA in living cells enabled the isolation of functional ventricular CMs from differentiating mESCs with high specificity and efficiency.

DISCUSSION

Over the past decade, there has been notable advancement in the methodologies for generating PSCs (Takahashi et al., 2007; Takahashi and Yamanaka, 2006) and producing CMs from PSCs, raising the prospects of using stem-cell-derived CMs for cardiac repair (Laflamme et al., 2007; Yang et al., 2008). However, all reported CM differentiation protocols to date can generate only heterogeneous CMs mixed with other cell populations. Although several recent studies reported non-genetic methods for isolating general CMs (Dubois et al., 2011; Hattori et al., 2010), these methods still generate heterogeneous CMs, not chamber-specific CMs. Given the major role of ventricular CMs for cardiac contractile function, it is important to develop a non-genetic method to isolate ventricular CMs from differentiating PSCs for preclinical and clinical applications.

To address this unmet need, in this work, we designed MBs targeting IRX4, a ventricular CM-specific transcription factor, generated homogeneous ventricular-like CMs from mESCs without altering their genome, and demonstrated that this method yielded functional ventricular CMs with high specificity and efficiency. Specifically,

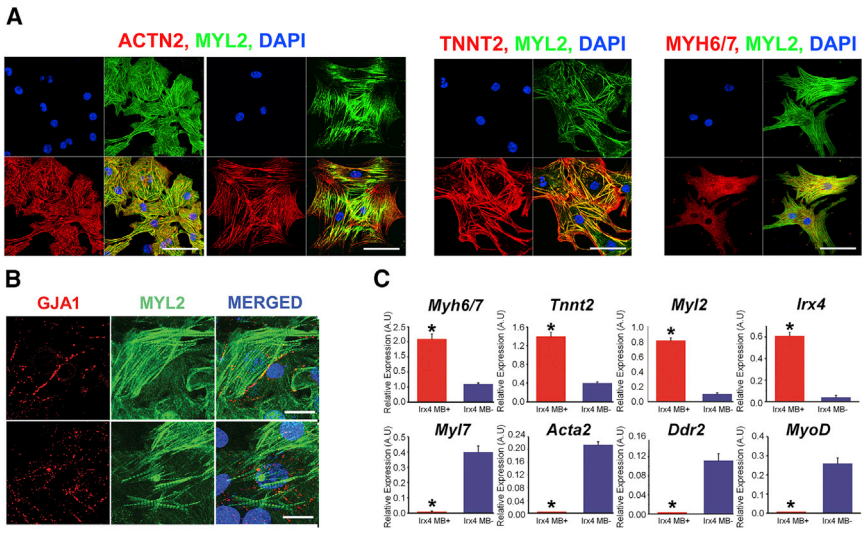

Figure 4. Characterization of Purified Ventricular CMs through IRX4-2 MBs

(A) Immunocytochemistry for ACTN2, TNNT2, and MYH6/MYH7 on IRX4-2-MB-positive cells isolated from cardiomyogenically differentiated mESCs. Scale bars, 20 μm.

(B) Expression of GJA1 determined by immunocytochemistry on IRX4-2-MB-positive cells isolated from cardiomyogenically differentiated mESCs. Scale bars, 50 μm.

(C) mRNA expression of cardiac (*Myh6/Myh7* and *Tnnt2*), ventricular (*Myl2* and *Irx4*), atrial (*Myl7*), and non-cardiac genes (*Acta2*, *Ddr2*, and *MyoD*) in IRX4-2-MB-positive and -negative cells measured by qRT-PCR. y axis represents relative mRNA expression of target genes to GAPDH. *$p < 0.05$ compared to in IRX4-2-MB-negative cell group. Data are represented as mean ± SEM. All experiments were performed on three independent biological replicates.

nucleofection-based delivery of MBs targeting the *Irx4* mRNA followed by FACS sorting enabled efficient enrichment of ventricular CMs from differentiating mESCs with 92% purity. In electrophysiological studies, approximately 98% of these MB-purified CMs demonstrated ventricular-CM-like action potentials and Ca^{2+} oscillations, indicating that they are functionally intact ventricular CMs. These cells showed coordinated contraction and maintained their phenotype for more than 2 weeks in culture.

Our study demonstrates that specific cells could be isolated with high specificity by targeting the mRNA of a transcription factor using MBs. This marks a significant advance of the method we developed recently, where the use of MBs targeting the mRNA of a structural protein (MYH) allowed sorting of general CMs from differentiating human and mouse PSCs (Ban et al., 2013). Since the mRNA expression of a transcription factor is usually much less abundant than that of a structural protein, it was very challenging to apply the MB-based method for the isolation of these specific cells. In fact, we initially designed MBs targeting another transcription factor, NKX2.5, but the MB signal level was not high enough for isolating CMs using FACS. Another major challenge was to identify an optimal delivery method to internalize a large amount of MBs (e.g., > 2,000 per cell) in order to generate a sufficiently high fluorescence signal when hybridized to target mRNAs. We tested quite a few different methods to deliver MBs into living cells, including the use of Streptolysin O, Lipofectamin 2000, Lullaby, microinjection, and nucleofection, and found that nucleofection with a specific buffer solution induced the maximal target mRNA detectability with minimal cytotoxicity (data not shown). We and others have found that after delivery into living cells, MBs do not affect the expression of the target mRNA or other mRNAs (Rhee and Bao, 2009), and they degrade within a few hours so that their effects on cell viability and cell functionality are negligible (Ban et al., 2013; Chen et al., 2008; Rhee and Bao, 2009; Rhee et al., 2008; Santangelo et al., 2006). Even with repetitive delivery of MBs, we did not observe phenotypic or functional changes of cells, as evidenced by the unaffected spontaneous contraction and the results of immunocytochemistry assays shown in this study.

Other RNA detection methods, such as the SmartFlare system (Halo et al., 2014; Lahm et al., 2015; Prigodich et al., 2012) and ratiometric bimolecular beacons (RBMB) (Chen et al., 2010; Zhang et al., 2013), have recently been developed. According to the published reports, both systems can generate sufficient and specific signals to be able to identify less abundant mRNA transcripts (Chen et al., 2010; Lahm et al., 2015). In addition, the cellular delivery of the SmartFlare system is generally easy due to the natural cellular uptake of the nanoparticles (Halo et al., 2014; Lahm et al., 2015; Prigodich et al., 2012). Nevertheless, the major advantages of an MB-based method over these two methods are the entropic bonus of a single molecule system and the ability to rapidly iterate design parameters. Since a standard MB is a single-molecule system, the enthalpy of the stem can be significantly lower than the SmartFlare or RBMB systems while still generating similar binding affinities for the target mRNA (Chen et al., 2008; Heyduk and Heyduk, 2002). In addition, there are a multitude of online software tools that predict single-stranded RNA structure. The RBMB system requires a more complicated two-molecule simulation,

and the SmartFlare system requires both a competitive binding calculation to be performed and the effect of steric hindrance to be considered due to the relatively large delivery particle.

We believe that the production of homogeneous and functional PSC-derived ventricular CMs using a non-transgenic approach will open new avenues for basic research and clinical applications. First, a pure population of ventricular CMs generated by the MB-based method offers a safer and more effective option for cell therapy and tissue engineering compared to the use of mixed populations of PSC-derived CMs, which are more likely to cause abnormal electrical activity (Liao et al., 2010) or less efficient contractile function (van Laake et al., 2008). From a research perspective, the MB-purified ventricular CMs represent a powerful in vitro tool for disease investigation and drug discovery. They can be used as better-defined in vitro model systems for genetic or idiopathic cardiac diseases such as long QT syndrome (Itzhaki et al., 2011; Moretti et al., 2010). They can also serve as an in vitro model to test chamber-specific effects of candidate cardiac drugs (Liang et al., 2013). These purified CMs will yield more accurate genetic and epigenetic information through high-throughput sequencing techniques. We anticipate that this MB-based cell-sorting method can be adopted for isolating other cardiac cells, such as nodal cells and atrial CMs, and has the potential to be used in isolating other cell types from differentiating PSCs, such as neuronal cells and pancreatic β cells.

EXPERIMENTAL PROCEDURES

MB Synthesis and Characterization

Three IRX4 MBs were synthesized by MWG Operon with high-pressure liquid chromatography (HPLC) purification (Table 1) (Ban et al., 2013). IRX4 MBs were re-suspended in nuclease-free PBS buffer (pH 7.4) to minimize buffer incompatibility with cells. IRX4 MBs were tested against synthetic 20- to 30-bp complementary sequences in PBS solution to verify their activity. To demonstrate specificity, MBs were also tested against synthetic targets with 6-bp mismatches.

Mouse ESC Culture and Differentiation

mESCs (J1) were maintained as described previously (Ban et al., 2013). To differentiate mESCs into cardiac lineage, an embryoid body method was used with some modifications. More details concerning the materials and methods can be found in the Supplemental Information.

Flow Cytometry

After nucleofection, cells were centrifuged at 1,500 rpm for 2 min, re-suspended in DMEM/F12 basal media, and maintained on ice for 20 min to recover. Cells were then analyzed by C6 Flow Cytometer (BD Biosciences) or sorted using a BD FACS Aria II cell sorter (BD Biosciences). MB signal was recorded using a 561-nm laser with a 585/15-nm emission filter to optimally excite and detect Cy3. For MB experiments, negative control MB (Table 1), whose loop sequence was generated using "random walk" and does not match with any mRNA sequence in the entire mouse genome, was used as a negative control for gating. For intracellular flow cytometry (TNNT2 and MYL2) analyses, isotype control antibodies were used as negative controls for gating. Data were analyzed using FlowJo software (Treestar).

Cell Viability Assay

FACS-sorted cells were resuspended in 1 ml of flow cytometry staining buffer and 5 μl of PI staining solution (Sigma) to each sample just prior to analysis. Then it was mixed gently and incubated for 1 min in the dark. PI fluorescence was determined by C6 Flow Cytometer (BD Biosciences) using the FL-2 channel at 488-nm laser illumination. Finally, the obtained results were compared to unstained cells and single-color positive controls.

Immunocytochemistry

Cells were fixed with 4% paraformaldehyde for 10 min at room temperature, washed twice with PBS, and permeabilized with 0.1% or 0.5% Triton X-100 in PBS for 10 min. Samples were then blocked with 1% BSA in PBS for 60 min at room temperature and incubated with anti-Actn2 (Sigma, #A7811; 1:100), mouse anti-Tnnt2 (Thermo, #MS295P1; 1:100), anti-Myl2 (Proteintech Group, #55462-1-AP; 1:100) or Gja1 (BD, #610062; 1:100) at 4°C overnight. The cells were washed three times with 1% Tween 20 in PBS and incubated with anti-mouse immunoglobulin G (IgG)-Alexa Fluor 594 (Thermo, #A-11005; 1:1,000) or anti-rabbit IgG-Alexa Fluor 488 (Thermo, # A-11008; 1:1,000) in PBS for 1 hr at room temperature. DAPI was used for nuclear staining. The samples were visualized under a fluorescent microscope (Nikon) and a Zeiss LSM 510 Meta confocal laser scanning microscope and LSM 510 Image software (CLSM, Carl Zeiss).

qRT-PCR

Total RNA was prepared with the RNeasy Plus Mini Kit (Qiagen) according to the manufacturer's instructions. The extracted RNA (100 ng to 1 mg) was reverse transcribed into cDNA (reverse transcription) via Taqman reverse transcription reagents, including random hexamers, oligo (dT), and MultiScribe MuLV reverse transcriptase (Applied Biosystems). qPCR was performed on a 7500 Fast Real-Time PCR system (Applied Biosystems) using Fast SYBR Green master mix (Applied Biosystems). All annealing steps were carried out at 60°C. Relative mRNA expression of target genes was calculated with the comparative CT method. All target genes were normalized to *Gapdh* in multiplexed reactions performed in triplicate. Differences in CT values (ΔCT = CT gene of interest − CT Gapdh in experimental samples) were calculated for each target mRNA by subtracting the mean value of *GAPDH* (relative expression = $2^{-\Delta CT}$) (Kim et al., 2010). Information on primer sets (Eurofins) used in this study is listed in Table S1.

Intracellular Calcium Imaging

For calcium (Ca^{2+}) imaging, IRX4-2-MB-based purified cells ESC-CMs were plated on glass coverslips and were loaded with 5 μM

fluo4 AM for 15 min in culture medium. Coverslips with cells were transferred to a temperature-controlled chamber on an Olympus Fluoview 1000 confocal microscope and washed with physiologic salt solution (Tyrode's) for 20 min for de-esterification of the dye. Experiments were done at 35°C. Linescan images were taken for cells showing calcium cycling. Calcium transients were analyzed using Clampfit software (Molecular Devices), and measures parameters such as amplitude, rise time from half amplitude to peak, and decay time from peak to half amplitude were averaged for 5–10 beats for each cell.

Action Potential Measurement

For intracellular AP recording, both IRX4-2-MB-positive and -negative cells were transferred and cultured on 0.1% fibronectin-coated glass bottom microwell dishes for 7 to 14 days. Next, the 35-mm dishes were mounted on an inverted microscope (Olympus IX71) and heated by a heating/cooling bath temperature controller (DTC-200, Dagan Corporation). The cells were perfused with Tyrode's solution containing (mmol/L) 140 NaCl, 5.4 KC1, 1 MgCl2, 10 HEPES, 10 glucose, 1.8 $CaCl_2$ (pH 7.4) with NAOH 37°C. Glass microelectrodes were fabricated from borosilicate glass (PG52151-4, World Precision Instruments) and pulled on a P-87 Flaming/Brown puller (Sutter Instrument Company). The tip resistance of the microelectrode was 40–80 MΩ when filled with a 3 mol/L KCl solution. Intracellular recordings of membrane potential were performed using an EPC 7 amplifier (List Medical) in current clamp mode at 37 ± 0.5°C. The junction potential between the microelectrode solution and the bath solution was adjusted to zero, and the microelectrodes' capacitance was compensated. Individual cells were impaled with the sharp microelectrodes, and the spontaneous APs were filtered at 10 kHz and digitized on a computer at 10 kHz. APs were analyzed using Origin 6.0 software (Microcal).

MEA Recordings

Both IRX4-2-MB-positive and -negative cells were examined using a MEA data acquisition system, a 64-channel Muse MEA system (Axion Biosystems). Thirty thousand cells were plated onto fibronectin-coated MEA chambers, and 3–5 days later, when cells were stabilized, MEA recording was performed. After recording, the data were analyzed using the AxIS software.

Statistical Analyses

All data were expressed as mean ± SEM. Kruskal-Wallis ANOVA test was used for the statistical analysis for a small number of samples. Values of $p < 0.05$ were considered to denote statistical significance. All statistical analyses were conducted using SPSS 20.0 (SPSS).

SUPPLEMENTAL INFORMATION

Supplemental Information includes Supplemental Experimental Procedures, four figures, one table, and two movies and can be found with this article online at http://dx.doi.org/10.1016/j.stemcr.2015.10.021.

AUTHOR CONTRIBUTIONS

K.B., B.W., K.-W.C., G.B., and Y.-S.Y. designed research; K.B., B.W., K.-W.C., S.K., M.-K.S., S.Y.K., J.S., and A.S. performed research; S.P.Y. and M.W contributed new reagents/analytic tools; K.W., B.W., K.-W.C., S.K., M.-K.S., and J.S. analyzed data; K.B., B.W., G.B., and Y.-S.Y. wrote the paper.

ACKNOWLEDGMENTS

We gratefully acknowledge the Emory Children's Pediatric Research Center flow cytometry core. This work was supported in part by the National Heart, Lung, and Blood Institute of the NIH as a Program of Excellence in Nanotechnology award (HHSN268201000043C to G.B. and Y.-S.Y.) and by grants from NIDDK (DP3DK094346 to Y.-S.Y.), NHLBI (R01HL127759 to Y.-S.Y. and R01HL088488 to M.W.), Faculty Research Assistance Program of Yonsei University College of Medicine 2015, and the Bio & Medical Technology Development Program of the National Research Foundation (NRF) funded by the Korean government (MSIP) (No 2015M3A9C6031514). K.B. is a recipient of an American Heart Association postdoctoral fellowship grant.

Received: September 14, 2014
Revised: October 29, 2015
Accepted: October 30, 2015
Published: December 8, 2015

REFERENCES

Ban, K., Wile, B., Kim, S., Park, H.-J., Byun, J., Cho, K.-W., Saafir, T., Song, M.-K., Yu, S.P., Wagner, M., et al. (2013). Purification of cardiomyocytes from differentiating pluripotent stem cells using molecular beacons that target cardiomyocyte-specific mRNA. Circulation *128*, 1897–1909.

Bao, Z.-Z., Bruneau, B.G., Seidman, J.G., Seidman, C.E., and Cepko, C.L. (1999). Regulation of chamber-specific gene expression in the developing heart by Irx4. Science *283*, 1161–1164.

Bizy, A., Guerrero-Serna, G., Hu, B., Ponce-Balbuena, D., Willis, B.C., Zarzoso, M., Ramirez, R.J., Sener, M.F., Mundada, L.V., Klos, M., et al. (2013). Myosin light chain 2-based selection of human iPSC-derived early ventricular cardiac myocytes. Stem Cell Res. (Amst.) *11*, 1335–1347.

Brundel, B.J.J.M., Henning, R.H., Ke, L., van Gelder, I.C., Crijns, H.J.G.M., and Kampinga, H.H. (2006). Heat shock protein upregulation protects against pacing-induced myolysis in HL-1 atrial myocytes and in human atrial fibrillation. J. Mol. Cell. Cardiol. *41*, 555–562.

Bruneau, B.G., Bao, Z.-Z., Tanaka, M., Schott, J.-J., Izumo, S., Cepko, C.L., Seidman, J.G., and Seidman, C.E. (2000). Cardiac expression of the ventricle-specific homeobox gene Irx4 is modulated by Nkx2-5 and dHand. Dev. Biol. *217*, 266–277.

Chan, L.L., Wilkinson, A.R., Paradis, B.D., and Lai, N. (2012). Rapid image-based cytometry for comparison of fluorescent viability staining methods. J. Fluoresc. *22*, 1301–1311.

Chen, A.K., Behlke, M.A., and Tsourkas, A. (2008). Efficient cytosolic delivery of molecular beacon conjugates and flow cytometric analysis of target RNA. Nucleic Acids Res. *36*, e69.

Chen, A.K., Davydenko, O., Behlke, M.A., and Tsourkas, A. (2010). Ratiometric bimolecular beacons for the sensitive detection of RNA in single living cells. Nucleic Acids Res. *38*, e148.

Claycomb, W.C., Lanson, N.A., Jr., Stallworth, B.S., Egeland, D.B., Delcarpio, J.B., Bahinski, A., and Izzo, N.J., Jr. (1998). HL-1 cells: a cardiac muscle cell line that contracts and retains phenotypic characteristics of the adult cardiomyocyte. Proc. Natl. Acad. Sci. USA *95*, 2979–2984.

Dubois, N.C., Craft, A.M., Sharma, P., Elliott, D.A., Stanley, E.G., Elefanty, A.G., Gramolini, A., and Keller, G. (2011). SIRPA is a specific cell-surface marker for isolating cardiomyocytes derived from human pluripotent stem cells. Nat. Biotechnol. *29*, 1011–1018.

Fujiwara, M., Yan, P., Otsuji, T.G., Narazaki, G., Uosaki, H., Fukushima, H., Kuwahara, K., Harada, M., Matsuda, H., Matsuoka, S., et al. (2011). Induction and enhancement of cardiac cell differentiation from mouse and human induced pluripotent stem cells with cyclosporin-A. PLoS ONE *6*, e16734.

Go, A.S., Mozaffarian, D., Roger, V.L., Benjamin, E.J., Berry, J.D., Borden, W.B., Bravata, D.M., Dai, S., Ford, E.S., Fox, C.S., et al.; American Heart Association Statistics Committee and Stroke Statistics Subcommittee (2013). Heart disease and stroke statistics—2013 update: a report from the American Heart Association. Circulation *127*, e6–e245.

Halo, T.L., McMahon, K.M., Angeloni, N.L., Xu, Y., Wang, W., Chinen, A.B., Malin, D., Strekalova, E., Cryns, V.L., Cheng, C., et al. (2014). NanoFlares for the detection, isolation, and culture of live tumor cells from human blood. Proc. Natl. Acad. Sci. USA *111*, 17104–17109.

Hattori, F., Chen, H., Yamashita, H., Tohyama, S., Satoh, Y.S., Yuasa, S., Li, W., Yamakawa, H., Tanaka, T., Onitsuka, T., et al. (2010). Nongenetic method for purifying stem cell-derived cardiomyocytes. Nat. Methods *7*, 61–66.

Heyduk, T., and Heyduk, E. (2002). Molecular beacons for detecting DNA binding proteins. Nat. Biotechnol. *20*, 171–176.

Huber, I., Itzhaki, I., Caspi, O., Arbel, G., Tzukerman, M., Gepstein, A., Habib, M., Yankelson, L., Kehat, I., and Gepstein, L. (2007). Identification and selection of cardiomyocytes during human embryonic stem cell differentiation. FASEB J. *21*, 2551–2563.

Hume, J.R., and Uehara, A. (1985). Ionic basis of the different action potential configurations of single guinea-pig atrial and ventricular myocytes. J. Physiol. *368*, 525–544.

Itzhaki, I., Maizels, L., Huber, I., Zwi-Dantsis, L., Caspi, O., Winterstern, A., Feldman, O., Gepstein, A., Arbel, G., Hammerman, H., et al. (2011). Modelling the long QT syndrome with induced pluripotent stem cells. Nature *471*, 225–229.

Kehat, I., Kenyagin-Karsenti, D., Snir, M., Segev, H., Amit, M., Gepstein, A., Livne, E., Binah, O., Itskovitz-Eldor, J., and Gepstein, L. (2001). Human embryonic stem cells can differentiate into myocytes with structural and functional properties of cardiomyocytes. J. Clin. Invest. *108*, 407–414.

Kim, H., Cho, H.-J., Kim, S.-W., Liu, B., Choi, Y.J., Lee, J., Sohn, Y.-D., Lee, M.-Y., Houge, M.A., and Yoon, Y. (2010). CD31+ cells represent highly angiogenic and vasculogenic cells in bone marrow: novel role of non-endothelial CD31+ cells in neovascularization and their therapeutic effects on ischemic vascular disease. Circ. Res. *107*, 602–614.

Kubalak, S.W., Miller-Hance, W.C., O'Brien, T.X., Dyson, E., and Chien, K.R. (1994). Chamber specification of atrial myosin light chain-2 expression precedes septation during murine cardiogenesis. J. Biol. Chem. *269*, 16961–16970.

Laflamme, M.A., and Murry, C.E. (2011). Heart regeneration. Nature *473*, 326–335.

Laflamme, M.A., Chen, K.Y., Naumova, A.V., Muskheli, V., Fugate, J.A., Dupras, S.K., Reinecke, H., Xu, C., Hassanipour, M., Police, S., et al. (2007). Cardiomyocytes derived from human embryonic stem cells in pro-survival factors enhance function of infarcted rat hearts. Nat. Biotechnol. *25*, 1015–1024.

Lahm, H., Doppler, S., Dreßen, M., Werner, A., Adamczyk, K., Schrambke, D., Brade, T., Laugwitz, K.-L., Deutsch, M.-A., Schiemann, M., et al. (2015). Live fluorescent RNA-based detection of pluripotency gene expression in embryonic and induced pluripotent stem cells of different species. Stem Cells *33*, 392–402.

Lee, M.Y., Sun, B., Schliffke, S., Yue, Z., Ye, M., Paavola, J., Bozkulak, E.C., Amos, P.J., Ren, Y., Ju, R., et al. (2012). Derivation of functional ventricular cardiomyocytes using endogenous promoter sequence from murine embryonic stem cells. Stem Cell Res. (Amst.) *8*, 49–57.

Lian, X., Hsiao, C., Wilson, G., Zhu, K., Hazeltine, L.B., Azarin, S.M., Raval, K.K., Zhang, J., Kamp, T.J., and Palecek, S.P. (2012). Robust cardiomyocyte differentiation from human pluripotent stem cells via temporal modulation of canonical Wnt signaling. Proc Natl Acad Sci U S A. *109*, E1848–1857.

Liang, P., Lan, F., Lee, A.S., Gong, T., Sanchez-Freire, V., Wang, Y., Diecke, S., Sallam, K., Knowles, J.W., Wang, P.J., et al. (2013). Drug screening using a library of human induced pluripotent stem cell-derived cardiomyocytes reveals disease-specific patterns of cardiotoxicity. Circulation *127*, 1677–1691.

Liao, S.-Y., Liu, Y., Siu, C.-W., Zhang, Y., Lai, W.-H., Au, K.-W., Lee, Y.-K., Chan, Y.-C., Yip, P.M.-C., Wu, E.X., et al. (2010). Proarrhythmic risk of embryonic stem cell-derived cardiomyocyte transplantation in infarcted myocardium. Heart Rhythm *7*, 1852–1859.

Marionneau, C., Couette, B., Liu, J., Li, H., Mangoni, M.E., Nargeot, J., Lei, M., Escande, D., and Demolombe, S. (2005). Specific pattern of ionic channel gene expression associated with pacemaker activity in the mouse heart. J. Physiol. *562*, 223–234.

Moretti, A., Bellin, M., Welling, A., Jung, C.B., Lam, J.T., Bott-Flügel, L., Dorn, T., Goedel, A., Höhnke, C., Hofmann, F., et al. (2010). Patient-specific induced pluripotent stem-cell models for long-QT syndrome. N. Engl. J. Med. *363*, 1397–1409.

Müller, M., Fleischmann, B.K., Selbert, S., Ji, G.J., Endl, E., Middeler, G., Müller, O.J., Schlenke, P., Frese, S., Wobus, A.M., et al. (2000). Selection of ventricular-like cardiomyocytes from ES cells in vitro. FASEB J. *14*, 2540–2548.

Ng, S.Y., Wong, C.K., and Tsang, S.Y. (2010). Differential gene expressions in atrial and ventricular myocytes: insights into the road of applying embryonic stem cell-derived cardiomyocytes for future therapies. Am. J. Physiol. Cell Physiol. *299*, C1234–C1249.

O'Brien, T.X., Lee, K.J., and Chien, K.R. (1993). Positional specification of ventricular myosin light chain 2 expression in the primitive murine heart tube. Proc. Natl. Acad. Sci. USA *90*, 5157–5161.

Popenda, M., Szachniuk, M., Antczak, M., Purzycka, K.J., Lukasiak, P., Bartol, N., Blazewicz, J., and Adamiak, R.W. (2012). Automated

3D structure composition for large RNAs. Nucleic Acids Res. *40*, e112.

Prigodich, A.E., Randeria, P.S., Briley, W.E., Kim, N.J., Daniel, W.L., Giljohann, D.A., and Mirkin, C.A. (2012). Multiplexed nanoflares: mRNA detection in live cells. Anal. Chem. *84*, 2062–2066.

Rhee, W.J., and Bao, G. (2009). Simultaneous detection of mRNA and protein stem cell markers in live cells. BMC Biotechnol. *9*, 30.

Rhee, W.J., Santangelo, P.J., Jo, H., and Bao, G. (2008). Target accessibility and signal specificity in live-cell detection of BMP-4 mRNA using molecular beacons. Nucleic Acids Res. *36*, e30.

Santangelo, P., Nitin, N., and Bao, G. (2006). Nanostructured probes for RNA detection in living cells. Ann. Biomed. Eng. *34*, 39–50.

Sasaki, D.T., Dumas, S.E., and Engleman, E.G. (1987). Discrimination of viable and non-viable cells using propidium iodide in two color immunofluorescence. Cytometry *8*, 413–420.

Shiba, Y., Fernandes, S., Zhu, W.-Z., Filice, D., Muskheli, V., Kim, J., Palpant, N.J., Gantz, J., Moyes, K.W., Reinecke, H., et al. (2012). Human ES-cell-derived cardiomyocytes electrically couple and suppress arrhythmias in injured hearts. Nature *489*, 322–325.

Takahashi, K., and Yamanaka, S. (2006). Induction of pluripotent stem cells from mouse embryonic and adult fibroblast cultures by defined factors. Cell *126*, 663–676.

Takahashi, T., Lord, B., Schulze, P.C., Fryer, R.M., Sarang, S.S., Gullans, S.R., and Lee, R.T. (2003). Ascorbic acid enhances differentiation of embryonic stem cells into cardiac myocytes. Circulation *107*, 1912–1916.

Takahashi, K., Tanabe, K., Ohnuki, M., Narita, M., Ichisaka, T., Tomoda, K., and Yamanaka, S. (2007). Induction of pluripotent stem cells from adult human fibroblasts by defined factors. Cell *131*, 861–872.

Tohyama, S., Hattori, F., Sano, M., Hishiki, T., Nagahata, Y., Matsuura, T., Hashimoto, H., Suzuki, T., Yamashita, H., Satoh, Y., et al. (2013). Distinct metabolic flow enables large-scale purification of mouse and human pluripotent stem cell-derived cardiomyocytes. Cell Stem Cell *12*, 127–137.

Tsourkas, A., Behlke, M.A., and Bao, G. (2002). Structure-function relationships of shared-stem and conventional molecular beacons. Nucleic Acids Res. *30*, 4208–4215.

van Laake, L.W., Passier, R., Doevendans, P.A., and Mummery, C.L. (2008). Human embryonic stem cell-derived cardiomyocytes and cardiac repair in rodents. Circ. Res. *102*, 1008–1010.

Wang, G.F., Nikovits, W., Jr., Bao, Z.-Z., and Stockdale, F.E. (2001). Irx4 forms an inhibitory complex with the vitamin D and retinoic X receptors to regulate cardiac chamber-specific slow MyHC3 expression. J. Biol. Chem. *276*, 28835–28841.

Xu, C., Police, S., Rao, N., and Carpenter, M.K. (2002). Characterization and enrichment of cardiomyocytes derived from human embryonic stem cells. Circ. Res. *91*, 501–508.

Yang, L., Soonpaa, M.H., Adler, E.D., Roepke, T.K., Kattman, S.J., Kennedy, M., Henckaerts, E., Bonham, K., Abbott, G.W., Linden, R.M., et al. (2008). Human cardiovascular progenitor cells develop from a KDR+ embryonic-stem-cell-derived population. Nature *453*, 524–528.

Zhang, Q., Jiang, J., Han, P., Yuan, Q., Zhang, J., Zhang, X., Xu, Y., Cao, H., Meng, Q., Chen, L., et al. (2011). Direct differentiation of atrial and ventricular myocytes from human embryonic stem cells by alternating retinoid signals. Cell Res. *21*, 579–587.

Zhang, X., Song, Y., Shah, A.Y., Lekova, V., Raj, A., Huang, L., Behlke, M.A., and Tsourkas, A. (2013). Quantitative assessment of ratiometric bimolecular beacons as a tool for imaging single engineered RNA transcripts and measuring gene expression in living cells. Nucleic Acids Res. *41*, e152.

Zuker, M. (2003). Mfold web server for nucleic acid folding and hybridization prediction. Nucleic Acids Res. *31*, 3406–3415.

Zwi, L., Caspi, O., Arbel, G., Huber, I., Gepstein, A., Park, I.-H., and Gepstein, L. (2009). Cardiomyocyte differentiation of human induced pluripotent stem cells. Circulation *120*, 1513–1523.